Journal of Advanced Research 31 (2021) 35–47

Contents lists available at ScienceDirect

Journal of Advanced Research

journal homepage: www.elsevier.com/locate/jare

Sleep/wake calcium dynamics, respiratory function, and ROS production in cardiac mitochondria

Engy A. Abdel-Rahman [a,b,c], Salma Hosseiny [a], Abdullah Aaliya [a], Mohamed Adel [a], Basma Yasseen [a,b], Abdelrahman Al-Okda [a], Yasmine Radwan [a], Saber H. Saber [a], Nada Elkholy [a], Eslam Elhanafy [a], Emily E. Walker [d,e], Juan P. Zuniga-Hertz [d,e], Hemal H. Patel [d,e], Helen R. Griffiths [f], Sameh S. Ali [a,b,*]

[a] Center for Aging and Associated Diseases, Zewail City of Science and Technology, Giza, Egypt
[b] 57357 Children's Cancer Hospital, Basic Research Department, Cairo, Egypt
[c] Department of Pharmacology, Faculty of Medicine, Assuit University, Assuit, Egypt
[d] Veterans Affairs San Diego Healthcare System, 3350 La Jolla Village Drive, San Diego, CA 92161, USA
[e] Department of Anesthesiology, University of California, San Diego, La Jolla, CA 92093, USA
[f] Swansea University, Swansea, Wales SA2 8PP, United Kingdom

GRAPHICAL ABSTRACT

Sleep/wake cycle-dependent differences in molecular parameters controlling mitochondrial ability to regulate cellular levels of calcium and associated ROS production.

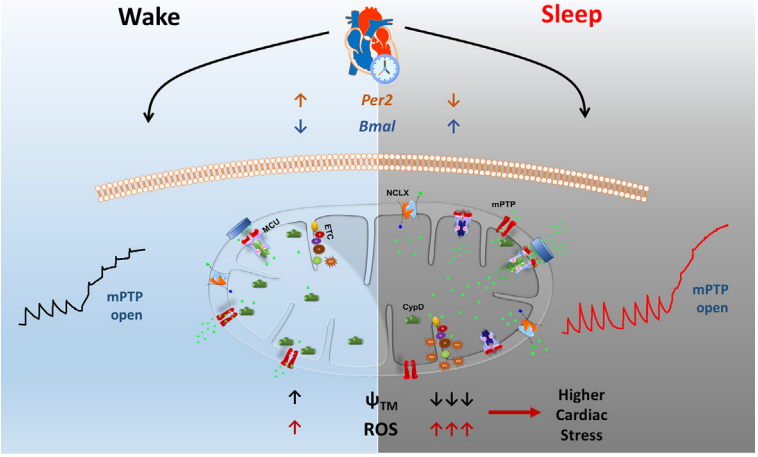

ARTICLE INFO

Article history:
Received 20 August 2020
Revised 24 November 2020
Accepted 7 January 2021
Available online 12 January 2021

ABSTRACT

Introduction: Incidents of myocardial infarction and sudden cardiac arrest vary with time of the day, but the mechanism for this effect is not clear. We hypothesized that diurnal changes in the ability of cardiac mitochondria to control calcium homeostasis dictate vulnerability to cardiovascular events.
Objectives: Here we investigate mitochondrial calcium dynamics, respiratory function, and reactive oxygen species (ROS) production in mouse heart during different phases of wake versus sleep periods.
Methods: We assessed time-of-the-day dependence of calcium retention capacity of isolated heart

Peer review under responsibility of Cairo University.
* Corresponding author at: Children's Cancer Hospital Egypt, 57357, Egypt.
E-mail address: sameh.ali@57357.org (S.S. Ali).

https://doi.org/10.1016/j.jare.2021.01.006

Keywords:
Heart
Mitochondria function
Calcium dynamics
Hydrogen peroxide
Diurnal
Clock genes

mitochondria from young male C57BL6 mice. Rhythmicity of mitochondrial-dependent oxygen consumption, ROS production and transmembrane potential in homogenates were explored using the Oroboros O2k Station equipped with a fluorescence detection module. Changes in expression of essential clock and calcium dynamics genes/proteins were also determined at sleep versus wake time points.

Results: Our results demonstrate that cardiac mitochondria exhibit higher calcium retention capacity and higher rates of calcium uptake during sleep period. This was associated with higher expression of clock gene *Bmal1*, lower expression of *per2*, greater expression of *MICU1* gene (mitochondrial calcium uptake 1), and lower expression of the mitochondrial transition pore regulator gene *cyclophilin D*. Protein levels of mitochondrial calcium uniporter (MCU), MICU2, and sodium/calcium exchanger (NCLX) were also higher at sleep onset relative to wake period. While complex I and II-dependent oxygen utilization and transmembrane potential of cardiac mitochondria were lower during sleep, ROS production was increased presumably due to mitochondrial calcium sequestration.

Conclusions: Taken together, our results indicate that retaining mitochondrial calcium in the heart during sleep dissipates membrane potential, slows respiratory activities, and increases ROS levels, which may contribute to increased vulnerability to cardiac stress during sleep-wake transition. This pronounced daily oscillations in mitochondrial functions pertaining to stress vulnerability may at least in part explain diurnal prevalence of cardiac pathologies.

Introduction

The onset of fatal cardiovascular events shows a clear time-of-the-day dependence with an apparent peak in the early hours of the morning. For example, myocardial infarction has a peak incidence between 06:00 AM and 12:00 noon [1]. There is also an early morning peak in atrial fibrillation, ventricular arrhythmias, cerebral infarction and sudden cardiac death [2–4]. Several cardiac parameters including heart rate and blood pressure exhibit circadian rhythmicity. Such circadian fluctuations aid the transition from rest/sleep to activity/wake and vice versa but pose significant risk in individuals who are susceptible to adverse cardiovascular events. Historically, these diurnal variations in cardiac function have been attributed to daily behaviors, specifically sleep-wake and fasting feeding cycles, and fluctuations in neurohumoral factors that include a catecholamine surge at wake time and a sudden rise in sympathetic activity [5–8]. However, recent evidence has emerged supporting the idea that an intrinsic circadian clock within the cardiovascular system mediates time of the day dependent variations in heart function and response to injury [9–11]. There are a few commonly accepted models explaining why this happens from neurohormonal loops (including cortisol and sympathetic nervous system) to metabolic and electrophysiological circadian oscillation within cardiomyocytes (reviewed in [12]). However, the precise mechanism by which the circadian clock system coordinates heart energy homeostasis is not fully understood.

In the heart, calcium ions (Ca^{2+}) play a central role in the regulation of energy balance and the coordination of myocardial contractile activity. Ca^{2+} homeostasis is disrupted in cardiovascular pathological states including heart failure and ischemia [13]. Mitochondrial Ca^{2+} uptake regulates cellular bioenergetics by enabling mitochondria to tune adenosine triphosphate (ATP) generation required for contraction and hence play a part in cardiac excitation–contraction coupling [14]. However, excessive mitochondrial Ca^{2+} accumulation causes respiratory inhibition, increased reactive oxygen species (ROS) production and induction of mitochondrial permeability transition pore (mPTP) opening, resulting in mitochondrial swelling, cytochrome *C* release and eventual apoptotic cell death [15]. In the suprachiasmatic nucleus (SCN) of rodents, time-of-day–dependent oscillations in levels of intracellular Ca^{2+} have been reported [16–20]. In addition, multiple Ca^{2+} channels within mouse brain and the L-type voltage gated Ca^{2+} channels (L-VGCCs) within embryonic chick hearts are regulated by the circadian clock [21,22]. A previous study detected weak rhythms in intracellular calcium levels in dispersed cardiomyocytes [23]. To the best of our knowledge, no study has assessed whether the mitochondrial Ca^{2+} dynamics in the heart oscillate during the day and how this oscillation, if present is synchronized with the mitochondria function and ROS homeostasis.

Our goal in this study is to analyze subtle sleep/wake cycle differences in mitochondrial calcium dynamics, mitochondrial function, and ROS homeostasis in mice heart using an array of sensitive techniques. Our results highlight inherent diurnal oscillation in mitochondrial calcium dynamics that is correlated with the circadian rhythmicity of mitochondrial function and ROS homeostasis in the heart. Understanding the complex interactions between circadian rhythms and mitochondrial calcium dynamics in the heart may provide insight into potential preventative and therapeutic approaches for susceptible populations.

Materials and methods

Animals

Young (6–8 weeks) C57BL6 male mice were purchased from Misr University for Science and Technology (Cairo, Egypt) and were certified to be purchased originally from Charles River Laboratories (U.S.A). Mice were housed in Zewail City animal facility until sacrificed. Animals were divided into two subgroups housed in normal or reversed light–dark cycles for at least 6–8 weeks before being used for experiments, with lights on (Zeitgeber cue; ZG 0) at 8:00 am and off at 8 p.m. (ZG 12). Animals sacrificed around ZG 0, ZG 16, and ZG 20 are considered awake and those sacrificed around ZG 4, ZG 8, and ZG 12 are considered asleep [22]. All animals were maintained in temperature-controlled rooms, with free access to water and standard laboratory rodent chow. Pairs of animals (one normal vs. one reversed light/dark cycle) were euthanized at 8 a.m., 12 p.m., or 4 p.m., by exposure to over dose of isoflurane followed by cervical dislocation. All animal work was carried out in adherence to the National Institutes of Health guide for the care and use of Laboratory animals (NIH Publications No. 8023, revised 1978) and was approved by Zewail City Administration. Animal studies conducted at UCSD were approved by the VA San Diego Healthcare System Institutional Animal Care and Use Committee (Protocol # A13-005).

Animals utilized in the study were divided into 3 groups, the first group involved 36 animals used for circadian profiles including 6 animals per time point (every 4 h) and used for mitochondrial metabolic and calcium dynamics studies. For sleep/wake gene expression profiles by qPCR comparisons, 6 mice were sacrificed

at 8 a.m. (ZG 0) and another 6 mice were sacrificed at 12 p.m. (ZG 4) and hearts were stored in the −80 °C until analyzed. The third group was devoted to explore the effect of quercetin treatment on mitochondrial ROS production, respiratory parameters, and calcium dynamics. This group included heart tissue from a total of 12 mice analyzed either at ZG 0 (N = 6) or ZG 4 (N = 6). The total number of animals euthanized in this study is 60 mice. The outcome measures or phenomena being measured are variable and large sample sizes are necessary for statistically valid sampling. Based on our previously published work, we estimate error around 10% SD when using n = 6–8 per group for 10–15% expected conditional effects. With type 1 error of 5% (alpha) and type 2 error (beta) 0.2, we calculated that the minimum necessary number of animals to reach significance is ~ 6 per condition.

Online power calculators were used to calculate the figures provided; e.g. http://powerandsamplesize.com/Calculators/Compare-2-Means/2-Sample-1-Sided.

Measurements of mitochondrial respiratory activities

After cervical dislocation, whole heart was dissected and immersed in ice-cold mitochondrial respiration medium, MIR05 containing 110 mM sucrose, 60 mM K-lactobionate, 0.5 mM EGTA, 1 g/liter BSA essentially fatty acid free, 3 mM MgCl2, 20 mM taurine, 10 mM KH2PO4 and 20 mM HEPES adjusted to pH 7.1 at 37 °C. Tissues were then transferred to a filter paper to remove excess liquid. A wet weight (1.4 mg of left atrium) was determined with a microbalance. Tissues were then transferred into Eppendorf tubes containing 2 ml of ice-cold, fresh MIR05 buffer. Using a pair of sharp forceps, tissues were cut into small pieces and transferred with the medium into an FT500-PS Shredder Pulse Tube for use with the PBI- shredder (Oroboros Instruments, Innsbruck, Austria). Tissue-dependent homogenization was then carried out according to the manufacturer's instructions.

Mitochondrial respiratory assessment and hydrogen peroxide production were carried out at 37 °C using the high-resolution respirometry system O2k (Oroboros Instruments, Innsbruck, Austria) in 2-ml chambers as previously described [24,25]. Before starting the experiment, calibration at air saturation versus zero oxygen was performed by allowing the respiration medium, MIR05 to equilibrate with air in the oxygraph chambers and stirred at 540–560 rpm for 30–40 min, until a stable signal was detected. 2 ml of heart (1.4 mg) homogenate was then added to each chamber, and tissues were permeabilized by the addition of saponin (50 μg/ml). Horseradish peroxidase (1 U per ml) and Amplex UltraRed fluorescent dye (10 μM), were then added, and the substrate–uncoupler–inhibitor titration (SUIT) protocol was performed as follows: Pyruvate Malate Glutamate (PMG) → ADP (D) → Succinate (S) → Oligomycin (O) → Carbonyl cyanide m-chlorophenyl hydrazone (CCCP) → Rotenone (R) → Antimycin A (Ama) → N,N,N',N'-tetramethyl-p-phenylenediamine/Ascorbate (TMPD/Asc). The rates of oxygen consumptions were calculated as the negative time derivative of oxygen concentration. Electron transport through complex I and III was abolished by adding rotenone (0.5 μM) and antimycin A (2.5 μM), respectively. The rate of hydrogen peroxide (H_2O_2) formation was detected in parallel to oxygen consumption in the same sample. Horseradish peroxidase (HRP) and Amplex UltraRed fluorescent dye were utilized with 525 nm excitation wavelength and 587 nm fluorescence detection wavelength. Signals were calibrated using known amounts of hydrogen peroxide that were exogenously added by the end of each run. Data acquisition and analysis were performed with the DatLab® software, version 4.3 (Oroboros Instruments). Oxygen consumption rate (OCR) and rate of H_2O_2 formation were normalized to citrate synthase activity.

Isolation of mitochondria

Isolation of mitochondria from hearts of mice was performed according to the method described previously [26]. Briefly, the heart was homogenized in mitochondrial isolation buffer containing (30 mM sucrose, 10 mM HEPES, pH 7.2, 0.2 mM EDTA, 1 mg/ml fatty acid free BSA) at 4 °C. Mitochondria were isolated by differential centrifugation. A Bradford assay was performed to determine protein concentrations that were used for normalization.

Calcium retention capacity (CRC) in isolated mitochondria

In a 96 well plate, 20 ~ 25 μg of isolated mitochondria were suspended in a total volume of 200 μL of assay buffer (adjusted to pH 7.4) containing (20 mM HEPES, 125 mM KCl/KOH, and 2 mM KH_2PO_4), followed by the addition of rotenone (0.5 μM) and succinate (10 μM). Calcium Green 5 N (1 μM) was then added and incubated for 5 min at room temperature. Successive pulses of Ca^{2+} (20 μM) were injected using programmable micro-infusion pump (BMG Labtech, Germany) every 30 sec to the energized mitochondria until a plateau of fluorescence was detected. The Calcium Green fluorescence was measured in a FLUOstar omega plate reader (BMG Labtech) using an excitation/emission wavelength of 506/532 nm respectively. Parameters pertaining to mitochondrial calcium dynamics were analyzed as follows: Rates of calcium uptake by mitochondria were estimated through the calculation of the slope of fluorescence decay following the abrupt rise in response to Ca^{2+} pulses. CRC were estimated as the overall amounts of infused Ca^{2+} that were necessary to cause mPTP opening as detected by sharp rise in the fluorescence of Calcium Green following mPTP and mitochondrial calcium release [27]. Amounts of Ca^{2+} retained inside mitochondria following a given number of Ca^{2+} pulses were calculated by subtracting the residual fluorescence minus the observed fluorescence after the addition of similar Ca^{2+} concentration in the absence of mitochondria. We calibrated the Ca^{2+} fluorescence signal using a Ca^{2+} calibration curve that was obtained in the absence of mitochondrial uptake due to uncoupling by FCCP. Increased fluorescence units resulting from 20 μM-boluses of Ca^{2+} (3 statistical replicates) were plotted against cumulative [Ca^{2+}].

Measurement of mitochondrial transmembrane potential

Heart tissues (1.4 mg) were homogenized and transferred to an O2k chamber. Tissues were permeabilized by the addition of saponin (50 μg/ml) and incubated with a lipophilic cationic fluorescence probe tetramethylrhodamine ethyl ester (TMRE) (0.5 μm) for 10 min. The membrane potential-dependent sequestration of TMRE in the mitochondria was assessed by measuring TMRE fluorescence using O2k-Fluorescence LED2-Module (Oroboros Instruments, Innsbruck, Austria) with excitation set at 490 nm and emission at 590 nm. Data were normalized to citrate synthase activity.

Quantitative real-time polymerase chain reaction (Q-RT-PCR)

Heart tissue section above apex from each mouse was collected for RNA isolation. Q-RT-PCR procedures were performed as previously described [28]· RNA was isolated using Trizol (Invitrogen) from heart biopsies of mice sacrificed at different time points. RNA purification was performed using RNeasy minikit (Qiagen) and cDNA reverse transcription was then carried out using High-capacity reverse transcription kit (Applied Biosystems). RT-PCR was carried out using primer-specific annealing temperature. PowerUp™ SYBR™ Green Master Mix (Applied Biosystems) was used to perform Q-RT-PCR on QuantStudio Real-Time PCR (QuantS-

Table 1
List of primers employed in the present study.

Name of genes	Forward primer (5′-3′)	Backward primer (5′-3′)
mβ-actin	CTGTCCCTGTATGCCTCTG	ATGTCACGCACGATTTCC
mGAPDH	GTTGTCTCCTGCGACTTCA	GGTGGTCCAGGGTTTCTTA
mND1	GCATCCGATATCAAGATGGATCG	CTTTAACCGTAACTCAGCCTTTTCA
mCypD	CAGACGCCACTGTCGCTTT	TGTCTTTGGAACTTTGTCTGCAA
mMICU1	AACAGCAAGAAGCCTGACAC	CTCATTGGGCGTTATGGAG
mEMRE	GTCAGTCATCGTCACTCGCA	CCCTGTGCCCTGTTAATCGT
mMICU2	CATGACACCCCGAGACTTCC	CCAGAGTGAGGTTTTGTGAGGA
mNCLXq	TCGCTGTGACTTTGTCAGGA	AAGCAGCCAGAAAACGTAGAGG
mMCUb	ATGCGTCGTTAATGCCAGGA	TGTTATTTCATCCTGTGGCTCC
mMCU	TACTCACCAGATGGCGTTC	GTCCTCTAACCTCTCCAC
mBmal	CAC TGT CCC AGG CAT TCC A	TTC CTC CGC GAT CAT TCG
mPer2	AAT CTT CCA ACA CTC ACC CC	CCT TCA GGG TCC TTA TCA GTTC

tudio 12 K Flex Real-Time PCR System). Levels of RNA were normalized to β-actin levels and estimated as delta-delta threshold cycle (ΔΔCT). All Q-RT-PCR reactions were carried out in triplicate. Primers used for RT-PCR are listed in Table 1.

Tissue harvest

4 months-old C57BL6 WT mice were used to analyze the circadian expression of heart mitochondrial proteins. For this purpose, hearts (n = 5 per time point) were collected immediately before the animal facility's lights turned on (at 6.00 AM) and 4hrs later (10.00 AM), corresponding to ZG = 0 and ZG = 4; respectively. Hearts were placed in mouse heart matrix, and apex was collected and snap-frozen in liquid nitrogen until total protein isolation.

Protein isolation and western blot analysis

Heart apex was pulverized in tissue pulverizer cooled in dry ice. Pulverized tissue was placed in 600 μL fresh lysis buffer (150 mM Na_2CO_3, supplemented with 1X protease/phosphatase inhibitor cocktail, pH 11) in a 2 ml Qiagen tube with one metal bead; samples were homogenized for 5 min at 50 oscillations/second in a Qiagen Tissuelyser Lt Bead Mill. Samples were let to settle on ice for 30 min and subsequent sonication (20 sec at 40% sonication intensity). 5 μg protein was loaded per well and resolved in 12% SDS gel. For immunoblot detection of mitochondrial and circadian proteins antibodies against ND1 (SAB4501927, Sigma), MCU (14997, Cell Signaling), MCUb (HPA048776, Sigma), MICU1 (HPA037480, Sigma), MICU2 (ab101564, Abcam), NCLX (ab136975, Abcam), EMRE (PAS23032, custom), BMAL1 (14020, Cell Signaling), Per2 (ab179813, Abcam), and GAPDH (2118S, Cell Signaling) were used at 1:1000 dilution. Band density analysis was performed with ImageJ software; all data is represented as total protein expression normalized by GAPDH.

Statistical analysis

Shapiro-Wilk normality test was carried out on all collected data sets and unless otherwise mentioned, all data sets were found to be significantly drawn (at the 0.05 levels) from normally distributed populations thus allowing mean comparisons using Student's *t* test. Welsh adjusted *t* test was used for relatively large sample sizes (N > 10) where equal variance is not assumed and/or whenever data with different sample sizes where compared. ANOVA followed by Tukey test was also employed for multiple groups' comparisons. Statistical significance was reached when $p < 0.05$. Chronographs depict means ± standard error of means (SEM) while Bar graphs and whisker plots show mean ± standard deviation (coefficient of variance at 1.5).

Results

Temporal profile of calcium dynamics in cardiac mitochondria

Mitochondria are a major player in dictating Ca^{2+} homeostasis and the Ca^{2+}-induced cellular response to stress. To determine whether sleep/wake cycle affects calcium uptake by mitochondria, the CRC assay has been performed using isolated mitochondria from murine hearts at different time points during the day. Between 4 and 12 successive 20-μM calcium pulses were applied to isolated mitochondria in the presence of 1 μM Calcium Green 5 N dye (which binds cytosolic Ca^{2+} to generate detectable fluorescence). Mitochondrial Ca^{2+} uptake leads to gradual decrease in the observed fluorescence, but the accumulation of the hydrated calcium ions leads to mitochondrial swelling and eventually burst; i.e. mPTP opening which results in a substantial increase in extramitochondrial Ca^{2+} concentration. Using this assay, Ca^{2+} retention capacity (CRC) was estimated as the amount of infused calcium that is necessary for triggering mPTP opening.

Representative traces for Ca^{2+} pulsing of cardiac mitochondria at ZG 0 (wake) and ZG 4 (sleep) are given in Fig. 1A. It is clear from Fig. 1A that cardiac mitochondria isolated during sleep period exhibit greater tolerance to calcium pulsing relative to those isolated from animals sacrificed during their wake periods. Fig. 1B shows the chronogram of CRC recorded every 4 h over 24 h period which demonstrate that mitochondria isolated from animals in their sleep and early wake periods exhibit greater CRC (ZG 4 vs. ZG 0; ZG 16; and ZG 20, $p < 0.01$, by ANOVA followed by Tukey test, N = 5–9 animals per time point as specified in the figure's legend). Overall, when time points were combined into two groups; i.e. wake and sleep groups, mitochondria from hearts of mice sacrificed during sleep and early wake period (ZG 4, 8, 12; total of 18 mice) exhibited significantly higher calcium retention capacity relative to wake (ZG 0, 16, 20; total of 21 mice) period (6.9 ± 0.5 vs. 4.34 ± 0.57 respectively; $p < 0.01$), suggesting delayed mPTP opening of cardiac mitochondria under Ca^{2+} overload during sleep (Fig. 1C).

Mitochondrial Ca^{2+} dynamics involve a delicate balance between Ca^{2+} influx and efflux that are controlled by multiple channels such as mitochondrial calcium uniporter (MCU) and antiporters (Na^+ dependent and independent Ca^{2+} exchangers) (Na^+/Ca^{2+} exchanger). mPTP opening is most likely to occur when relatively large amounts of Ca^{2+} are sequestered in mitochondria or when the uptake of Ca^{2+} is very fast while release is slow. Accordingly, the amount of Ca^{2+} sequestered by mitochondria and the rate of Ca^{2+} uptake were also studied (Fig. 2). An initial rapid spike in Calcium Green-5 N fluorescence intensity is detected when Ca^{2+} is added to isolated mitochondria, which was followed by a slower decrease in the fluorescence intensity, corresponding to mitochondrial Ca^{2+} uptake (Fig. 2A).

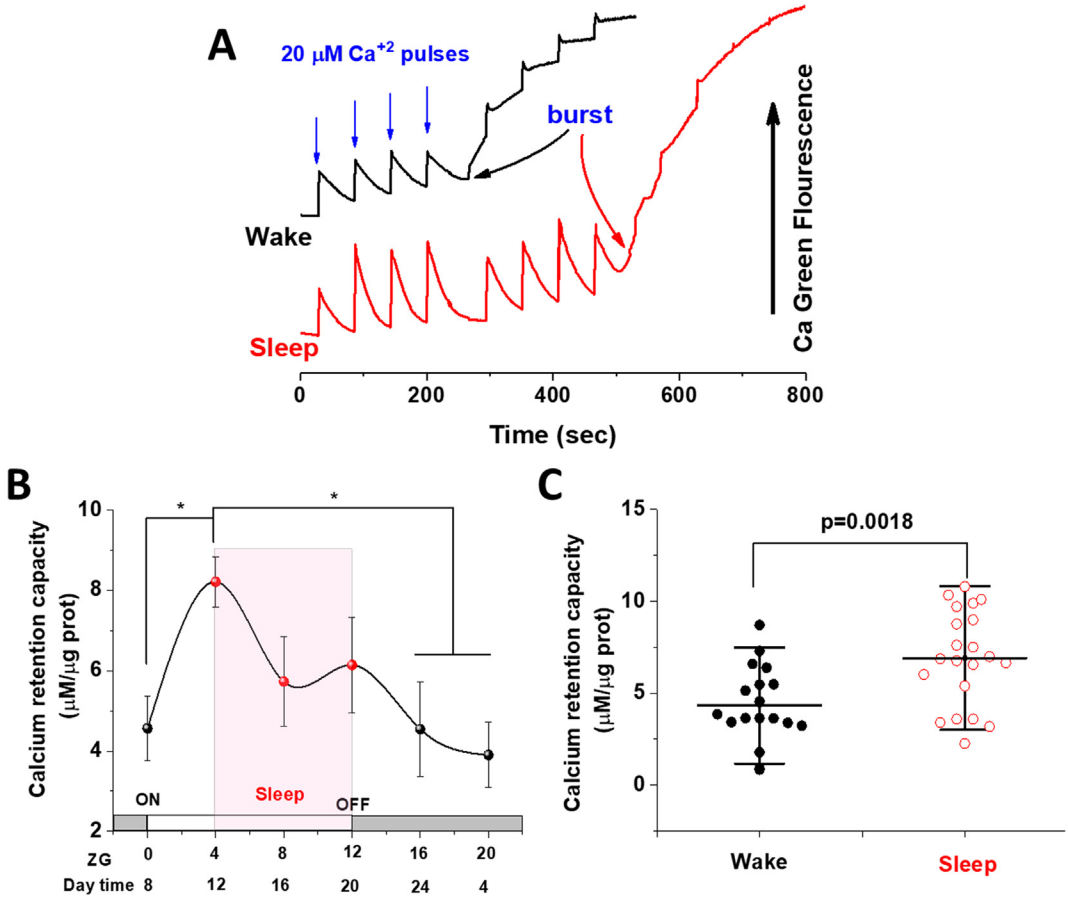

Fig. 1. Variation of the calcium retention capacity of cardiac mitochondria over the day. (A) Representative traces for calcium pulsing assay that is used to assess calcium retention capacity (CRC) of freshly isolated cardiac mitochondria from hearts of mice sacrificed at ZG 0 (Wake) and ZG 4 (Sleep) with arrows indicating successive infusions of 20-μM calcium pulses every 60 s in the presence of the low-affinity Calcium Green 5 N dye as detailed in the Methods' Section. (B) Chronogram displaying time of the day-dependent variations in CRC of cardiac mitochondria (μM Ca^{2+}/μg protein). n = 7, 9, 6, 6, 5, 6 animals time points ZG 0, 4, 8, 12, 16, 20; respectively. CRC was calculated for each time point as the sum of Ca^{2+} pulses taken-up by mitochondria prior to the induction of mPTP opening and mitochondrial burst marked by abrupt increase in fluorescence. (C) Comparing RCRs quantified for cardiac mitochondria isolated during wake period (mice sacrificed at ZG 0, 16, and 20, total of 21 mice) versus those sacrificed during sleep and early wake period (ZG 4, 8, and 12, total of n = 18 mice). p-values are calculated using ANOVA followed by Tukey test for means comparisons and are given for relevant conditions. Data are shown as mean ± SEM for (B) and mean ± SD for (C).

In our experiments, mitochondrial burst was rarely seen during the infusion of the first four Ca^{2+} pulses irrespective of the time of the day. Thus, the amount of Ca^{2+} sequestered by mitochondria after the first four 20 μM Ca^{2+} pulses was determined during sleep and wake periods. We calibrated the Ca^{2+} fluorescence signal using a Ca^{2+} calibration curve that was obtained in the absence of mitochondrial uptake (Fig. 2B). The dissociation constant (K_d) describes how tightly an indicator dye binds Ca^{2+} ions. The K_d corresponds to the concentration of Ca^{2+} at which half the dye molecules are bound with Ca^{2+} at equilibrium. K_d for Calcium Green 5 N, which is a low affinity indicator is 14 μM. It is recommended to employ Ca^{2+} concentration ranges between 0.1 and 10xK_d to maintain calcium determinations within the linear range of the calibration curve [29], which doesn't necessarily imply that the dye loses response above this range. The curve in Fig. 2B shows a non-linear behavior but still showed reproducible fluorescence response up to 200 μM. However, most of our recorded changes in [Ca^{2+}] used for rate calculations for individual pulses are below 20 μM which is well-within the linear response below 60 μM-[Ca^{2+}]. When we assessed the amounts of Ca^{2+} accumulated in cardiac mitochondria after adding the first 4 pulses of Ca^{2+} we observed a weak trend for higher calcium concentrations retained in mitochondria in the sleep group (2.59 ± 0.23 μM.μg^{-1} protein, sleep group vs. 1.88 ± 0.38 μM.μg^{-1} protein, wake group, p = 0.10, Fig. 2C).

To shed light on the inherent ability of mitochondria to handle calcium stress we analyzed the average rates of mitochondrial Ca^{2+} uptake (Supplementary Fig. S1) by calculating the slope of the initial phase of fluorescence decay as shown in Fig. 2A. Traces with clear pulses characterized by fluorescence rise followed by fluorescence decay (Ca^{2+} uptake), plateau (equilibrium), or even rise (release) prior to mPTP openings were considered in this analysis which is reflected in positive, zero, or negative rate values. We show in Supplementary Fig. S1.A the chronogram of the normalized rates of calcium uptake at various time points. Only ZG 4 showed statistically higher rates relative to ZG 8 and ZG 12 ($p < 0.05$). Yet, the rates of Ca^{2+} uptake calculated from the initial uptake phase for each of the first 4 pulses of Ca^{2+} during sleep and wake periods were not significantly different (1.10 ± 0.16 μM.min^{-1}.μg^{-1} protein during wake vs. 1.25 ± 0.20 μM.min^{-1}.μg^{-1} protein during sleep, Fig. S1.B). To evaluate the overall rate of calcium uptake for each pulse we followed the time after which the signal amplitude drops to half of its initial value [30]. Mean half-amplitude time determined at ZG 16 was significantly greater than all other time points including ZG 4 (Fig. 2D). When combined data from wake period was compared with those determined during

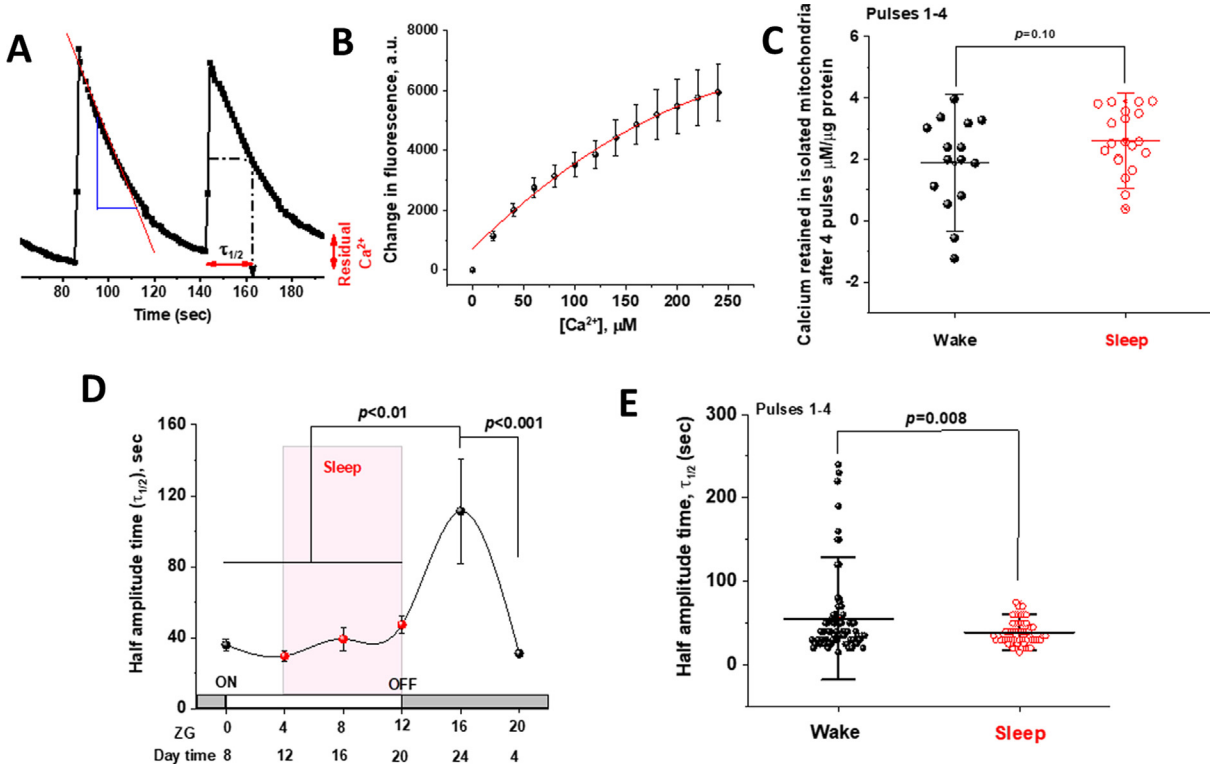

Fig. 2. Analysis of calcium dynamics in freshly isolated cardiac mitochondria reveals disparity in their ability to tolerate calcium stress during sleep versus wake periods. (A) Rates of mitochondrial Ca^{2+} uptake estimated by calculating the time taken for the decaying calcium fluorescence signal to reach half of the initial amplitude is denoted '$\tau_{1/2}$' (B) Ca^{2+} calibration curve constructed by plotting changes in fluorescence intensity following incremental additions of known Ca^{2+} concentrations on a buffer containing Calcium Green 5 N dye in the absence of mitochondrial uptake. (C) Mitochondria isolated from mice hearts during their sleep period showed a weak trend of increased sequestration of calcium following the first four 20-μM Ca^{2+} pulses relative to those isolated during the wake periods (p = 0.10, n = 15 and 20 mice for wake and sleep periods; respectively). Mitochondria-retained calcium was calculated by subtracting expected-minus-observed fluorescence intensities and conversion to concentrations using the calibration curve. (D) Chronogram depicting time-of-the-day dependence of $\tau_{1/2}$ (the time taken for calcium signals to decay to half of their initial amplitude). N = 7, 9, 6, 6, 5, 6 animals per time points ZG 0, 4, 8, 12, 16, 20; respectively. $\tau_{1/2}$ was determined for each of the first 4 pulses whenever observed. ZG 16 was significantly higher when compared with all other time points, p < 0.01 by one way ANOVA followed by Tukey test. (E) Data in panel D assembled in wake versus sleep groups and showed significantly lower $\tau_{1/2}$; i.e., faster calcium uptake by mitochondria isolated from animals sacrificed during sleep period. $\tau_{1/2}$ values were obtained for individual pulses observed and compared for the two groups by ANOVA followed by Tukey test, $p = 0.008$ (n = 18 and 21 mice for sleep and wake periods; respectively). Data are shown as mean ± SEM for (D) and mean ± SD for (B,C,E).

sleep period the former showed longer $\tau_{1/2}$; i.e. slower decay due to slower calcium uptake by mitochondria ($\tau_{1/2}$ = 55.6 ± 5.6 s during wake vs. 38.7 ± 1.7 s during sleep, $p = 0.007$, Fig. 2E). It appears from these data that the initial phase of calcium uptake during the first few seconds following each pulse shows a weak dependence on the time of the day while slower uptake starts to prevail later (>10 s) especially around ZG16. However, it is not clear at this stage how these observations relate to the ability of cardiac tissue to handle calcium stress at various times during the day.

Sleep/wake cycle-dependent expressions of clock, mitochondrial and Ca^{2+}- related genes in the heart

Our results so far demonstrate that Ca^{2+} dynamics in cardiac mitochondria are dependent on the time of the day with higher rates of calcium uptake and greater retention capacity observed during sleep. We then moved to explore how the observed functional characteristics in isolated mitochondria match with levels of genes encoding for proteins relevant to mitochondrial calcium machinery (MCU, MCUb (two subunits), MICU1, MICU2, EMRE, CypD, and NCLX) along with two important clock genes (Bmal1 and Per2); Fig. 3 A,B. We first asked how circadian clock gene expression in the heart is related to calcium rhythms in cardiac mitochondria. We monitored cardiac expression of the rhythmic clock genes Bmal1 and Per2 at ZG 0 (time point during wake period) and ZG 4 (time point during sleep period) (Fig. 3B). Bmal1 has been reported to be a main regulator of the Ca^{2+} circadian rhythms in neurons of the SCN of the hypothalamus [31]. As shown in Fig. 3B, cardiac expression of *Bmal*1 gene was significantly lower at ZG 0 in comparison with ZG 4 (0.71 ± 0.16 vs. 3.54 ± 1.3, p = 0.043; ANOVA test, n = 10 per group, Fig. 3B). The opposite trend was observed for the mRNA level of *Per*2 when going from ZG 0 to ZG 4 (2.3 ± 0.3 vs. 0.50 ± 0.06, p < 0.0001, Fig. 3B). The clock genes relative trends of changes are remarkably similar to previous reports including linking disturbance in their diurnal rhythms with cardiovascular risks [32]. We also detected significant differences in cardiac gene expression of NADH dehydrogenase (ND1, Ubiquinone) between ZG 0 and ZG 4 with higher level during sleep (Fig. 3B) indicating that diurnal changes in clock genes may also be associated with significantly detectable parallel changes in mitochondrial ETC complexes' biogenesis.

We then proceeded to explore diurnal variations in the expression levels of genes encoding for key regulators of mitochondrial calcium dynamics at ZG 0 and ZG 4 (illustrated in Fig. 3A and analyzed in Fig. 3B). Mitochondrial calcium uniporter (*MCU*) was reported to be the route for Ca^{2+} uptake into mitochondria. A regulatory subunit, mitochondrial calcium uniporter 1 (*MICU1*) has been recently shown to stimulate MCU activity [33]. We observed a non-significant difference in the level of gene expression of *MCU* between ZG 0 and ZG 4 in murine heart (1.20 ± 0.13 during wake vs. 1.0 ± 0.2 during sleep; n = 10 per group, Fig. 3B). However, cardiac *MICU1* expression was significantly lower at ZG 0, compared

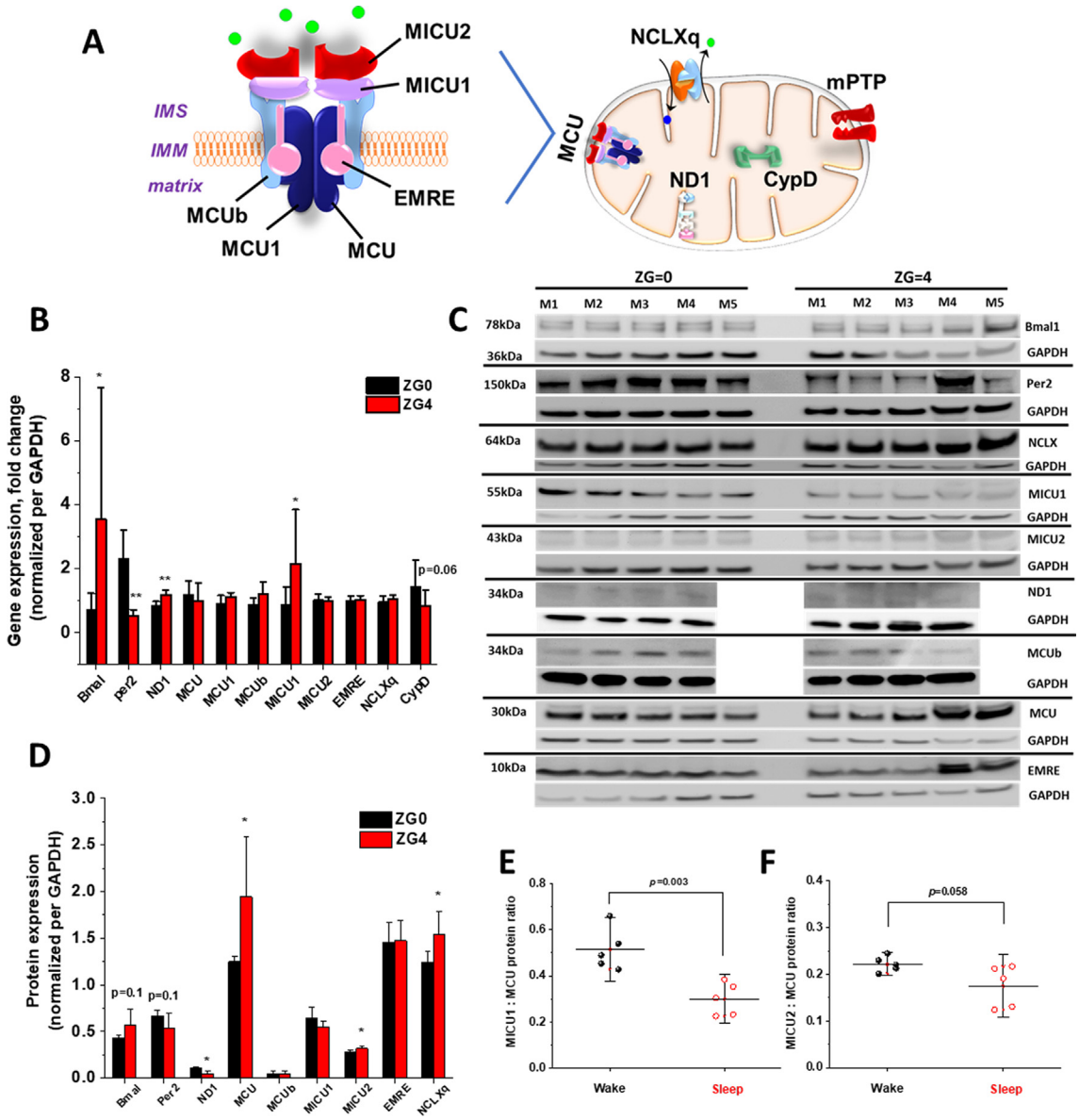

Fig. 3. Sleep/wake profiles of expressions of mitochondrial-, calcium-, and clock-related genes and proteins in mice hearts. (A) Schematic representation of mitochondrial calcium uniporter (MCU) Ca^{2+} channel showing subunits assessed in this work. Genes quantified include *Bmal*1; *Per*2; NAD dehydrogenase (*ND*1); *MCU* and subunits depicted; along with sodium/calcium exchanger channel (*NCLX*) and cyclophilin D (*CypD*). (B) Comparing cardiac gene expressions at ZG 0 versus ZG 4. The numbers of animals studied at each time point are n = 5 for ND1, MCU1, MCUb, MICU2, EMRE, and NCLX; n = 9 for MICU1 and CypD; and n = 10 for Bmal, Per2, and MCU. One way ANOVA followed by Tukey test was employed for comparisons of means, $p < 0.05$ (*), $p < 0.01$ (**) (C,D) Western blot detection of various proteins pertaining to clock and mitochondrial calcium dynamics in mouse hearts extracted at ZG0 versus ZG4 (quantified in D, n = 4 for ND1 and MCUb and 5 for other proteins, one way ANOVA followed by Tukey test, $p < 0.05$ (*) or $p < 0.01$ (**)). (E) MICU1 to MCU and MICU2 to MCU (F) ratios are calculated from levels of protein expression (n = 5 per group, data shown are Means ± SD).

to ZG 4 (0.86 ± 0.18 vs. 2.14 ± 0.54, $p = 0.047$; n = 9 and 10 animals, Fig. 3B). Increased expression in MICU1 is in tune with the higher rate of calcium uptake by cardiac mitochondria observed during sleep relative to wake period particularly under challenging mitochondria with higher [Ca^{2+}].

Because the process of opening of mPTP depends on the sensitivity of mPTP to Ca^{2+}, we examined the expression levels of cyclophilin D gene (*CypD*), which is the major sensor of Ca^{2+} and mPTP pore regulator [35,35]. Our results revealed that cardiac expression of CypD at ZG 0 showed a clear trend towards higher level relative to that at ZG 4 (1.44 ± 0.27 during wake vs. 0.84 ± 0.15 during sleep, $p = 0.06$; n = 9 and 10 animals; respectively, Fig. 3B), providing evidence for enhanced sensitivity of opening of mPTP to Ca^{2+} during wake period. This implies that during sleep, mitochondrial Ca^{2+} influx is facilitated by MICU1 subunit upregulation, but efflux might be hindered due to CypD downregulation.

Sleep/wake cycle-dependent expressions of clock and Ca^{2+}-related proteins in the heart

To extrapolate on the gene findings, we then moved to assess expression levels of various relevant proteins including MCU, MCUb, MICU1, MICU2, EMRE and NCLX in homogenized heart tissue collected either at ZG0 or ZG4 (Fig. 2C,D). Among those proteins, statistically significant increase in expression levels of MCU, MICU2 and NCLX were observed at ZG4 (Fig. 3C). Mitochondrial Ca^{2+} uptake behavior for a population of mitochondria within a tissue was elegantly shown to be dictated by the relative

abundance of MICU1 and MCU [36]. In the present work, we found that the MICU1:MCU protein ratio decreased significantly from 0.51 ± 0.04 to 0.29 ± 0.03 (n = 5 per group, p < 0.01) on going from wake (ZG0) to onset of sleep (ZG 4); upper panel of Fig. 3E. Similar trend that didn't reach statistical significance was observed for the MICU2:MCU ratio; lower panel of Fig. 3E. The trend towards lower ratio on the onset of sleep indicate relative abundance of MICU1-free uniporters that maybe compared with MICU1 loss of function or down-regulation/knock-out.

Ca^{2+} retention during sleep lowers mitochondrial oxidative phosphorylation (OXPHOS), dissipates transmembrane potential, and produces more ROS

Given that Ca^{2+} cycling and mitochondrial bioenergetics are interlinked [37], we followed the effect of sleep/wake cycle on mitochondrial bioenergetics in the heart. We evaluated mitochondrial respiration as oxygen consumption (Fig. 4 A&D), ROS production (Fig. 4 C&F) and transmembrane potential by O2k-Fluorometry utilizing the TMRE fluorescence assay (Fig. 4 B&E) in heart homogenate of 2–4-month-old male C57BL6 mice during sleep/wake cycle. The representative traces in Fig. 4 show that mitochondrial oxygen utilization and transmembrane potential are augmented in cardiac mitochondria during the wake period especially following the addition of succinate. This was associated with lower hydrogen peroxide (H_2O_2) flux in the wake group (Fig. 4C compared with Fig. 4F).

We followed the chronograms of oxygen consumption rate (OCR), transmembrane potential and H_2O_2 flux over 24 h in homogenized mouse hearts (Fig. 5 A-C; respectively). Furthermore, we compared OCR, transmembrane potential, and ROS flux that were pooled for time points during sleep against those during wake cycles (Fig. 5D-F). A strong trend of higher OXPHOS-II-dependent OCR during wake was observed (35.19 ± 6.07 for sleep (n = 26) vs. 59.35 ± 10.3 for wake (n = 29); p = 0.054, Fig. 5D). This was confirmed by the finding that cardiac mitochondria have significantly lower transmembrane potential during sleep period as compared to wake period (0.67 ± 0.06 for sleep vs 1.03 ± 0.12 for wake, p = 0.015 Fig. 5E). However, the rate of H_2O_2 production during OXPHOS-I + II in cardiac mitochondria is significantly higher during sleep compared to wake period (2.12 ± 0.19 for sleep vs. 1.49 ± 0.16 for wake, p = 0.014, Fig. 5F).

It is increasingly reported that Ca^{2+} and ROS flux are interlinked. Genetically encoded Ca^{2+} sensors, targeted to the mitochondria, enabled the use of fluorescence microscopy to show that quercetin, a well-described antioxidant, decreased mitochondrial [Ca^{2+}] [38]. A previous report [39] indicated that quercetin reduces cell swelling by regulating intracellular [Ca^{2+}]. We therefore investigated whether quercetin would prevent calcium accumulation in cardiac mitochondria observed during sleep period (Supplementary Fig. S2). In a representative subgroup (N = 4) of isolated heart homogenates we followed the effects of quercetin treatment on respiratory oxygen fluxes (Fig. S2.A) hydrogen peroxide and (Fig. S2.B) and followed the effect of addition of 100 μM quercetin on these parameters (quantified in Fig. S2.C&D). We also followed calcium uptake by isolated mitochondria during both wake and sleep cycles (Fig. S2.E&F). Our results indicated that quercetin effectively quenched ROS production in homogenized and permeabilized cardiac tissue while preserving oxygen consumption at ZG0. These effects were more pronounced in case of mitochondria isolated at ZG4. Quercetin also dramatically blocked calcium uptake in freshly isolated mitochondria especially at ZG0 (Fig. S2. F). That is, when CRC was measured for isolated mitochondria at ZG0 following their incubation with 100 μM quercetin for 5 min, no bursting mitochondria behavior was detected (n = 6; 4 showed staircase and 2 non-bursting responses) as compared with untreated mitochondria (n = 8; 6 bursting and 2 staircase responses). For those isolated at ZG4, more than half of the studied animals continued to exhibit mPTP opening with quercetin (4 out of 7) relative to untreated mitochondria. These results indicate that quercetin treatment of mitochondria isolated at ZG 4 was less protective against calcium overload.

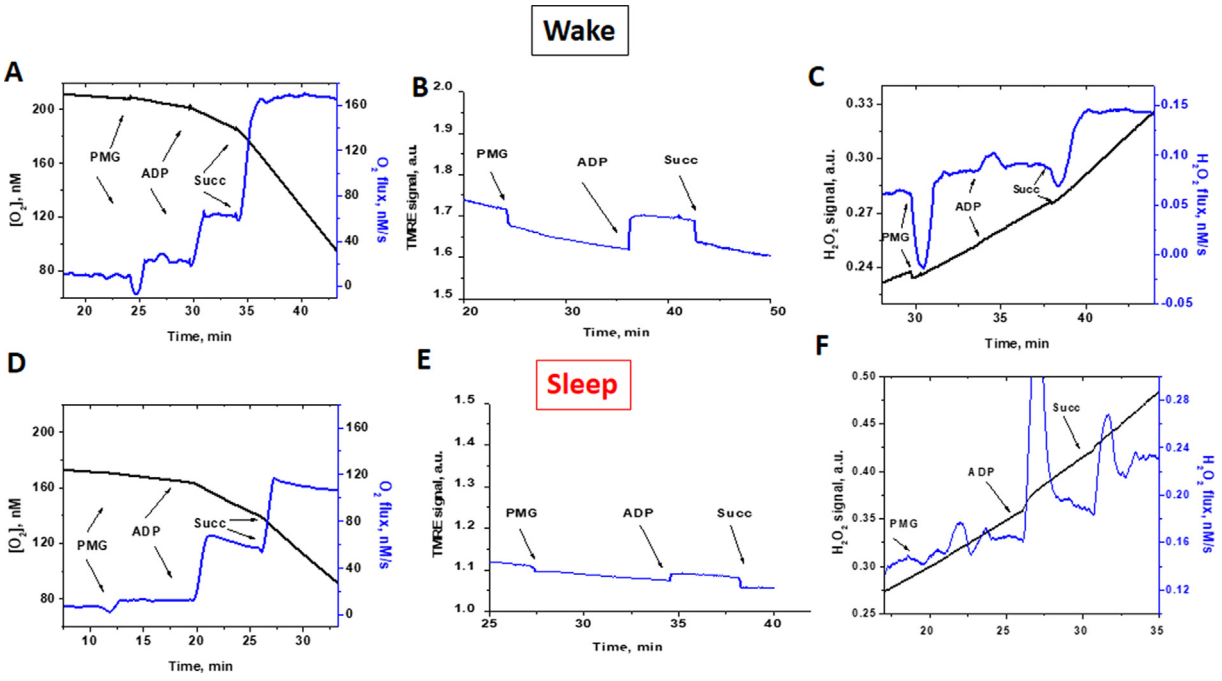

Fig. 4. Cardiac mitochondrial function is dependent on sleep/wake cycle. Comparison of sleep/wake cycle-dependent rates of mitochondrial oxygen consumption (A vs. D), transmembrane potential (B vs. E), and H_2O_2 production (C vs. F) in homogenized, saponin-permeabilized young mice heart. Representative traces illustrate ETC substrate-specific O_2 utilization (A&D) and H_2O_2 production (C&F) during Substrate-Uncoupler-Inhibitor Titration (SUIT) protocol in mice heart homogenate at ZG 0 (Wake) and ZG 4 (Sleep) (B&E). Representative traces of transmembrane potential in homogenized and saponin-permeabilized young mice heart at ZG 0 and ZG 4.

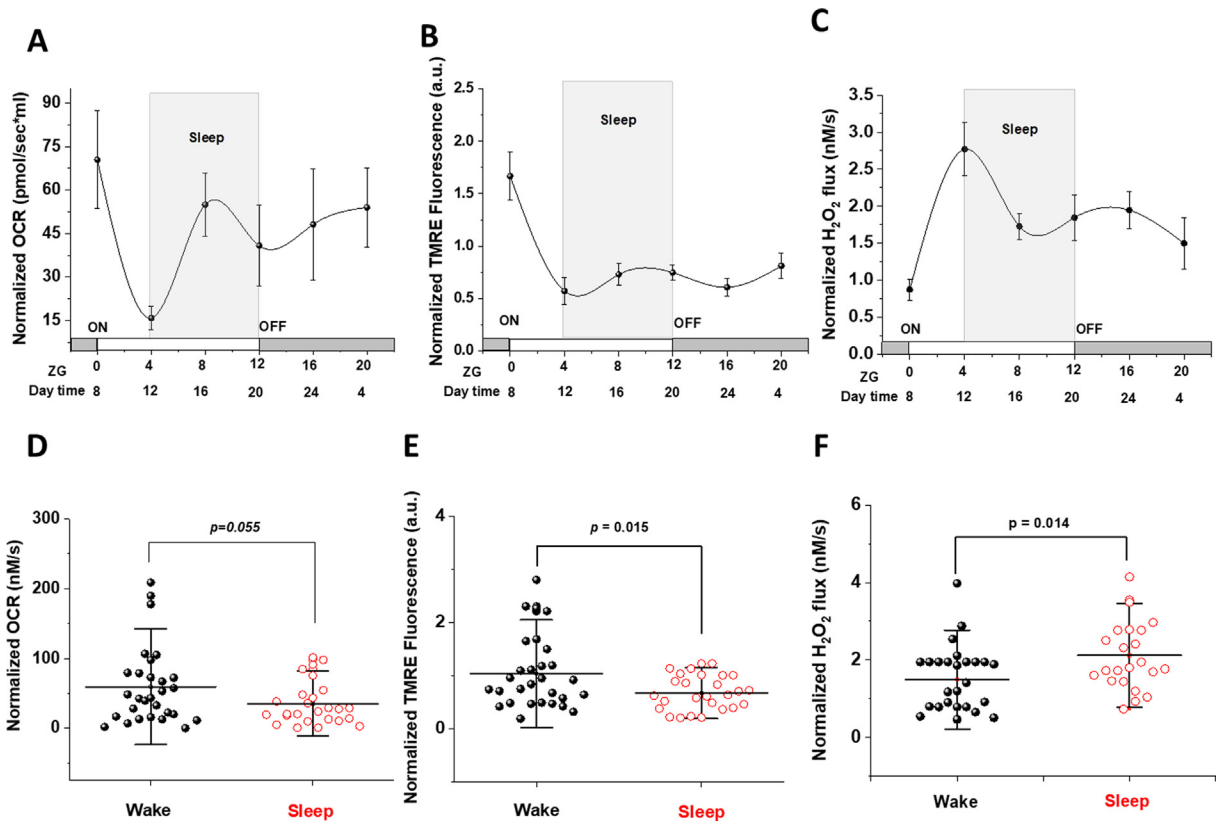

Fig. 5. Mitochondrial functions exhibit time of the day dependence in young mice hearts. Chronograms displaying time of the day quantified variations in OCR (A), TMRE fluorescence reflecting mTMP (B) and H_2O_2 flux per volume (C) over 24 h and normalized to citrate synthase activity in homogenized mice hearts (n = 12, 11, 9, 6, 8, 6 animals at ZG 0, 4, 8, 12, 16, 20; respectively). (D) Normalized rates of oxygen consumption in mice heart homogenate pooled to compare wake with sleep periods (p = 0.0549), (E) normalized TMRE fluorescence (p = 0.015), and (F) normalized H_2O_2 flux (p = 0.014) (from D to F, n = 26 for sleep and n = 29 for wake groups). Data are represented as mean ± SEM (A-C) and mean ± SD (D-F). Means comparisons were carried out using by ANOVA followed by Tukey test.

Discussion

Previous studies of the diurnal rhythmicity of cardiac physiology and associated risk for fatal cardiovascular events have not investigated either oscillations in cardiac mitochondrial calcium dynamics or their coupling with any circadian oscillations in mitochondrial bioenergetics and ROS homeostasis. Here we demonstrate for the first time that the heart mitochondrial CRC is significantly higher during sleep and is associated with, and may be regulated by, an increase in mitochondrial ROS production. In the utilized calcium pulsing protocol we employed very commonly used stimulating concentrations [41,41,42,43,44]. In human heart, it is known that the resting cytosolic [Ca^{2+}] is around 100 nM, but with each heart beat this level usually rises 10 times to be around 1 μM [45]. However, close proximity of the abundant intermyofibrillar mitochondria to the sarcoplasmic reticulum creates microdomains in which mitochondria maybe exposed to [Ca^{2+}] as high as > 20 μM [46]. In fact, the mitochondrial calcium uniporter, which is activated by calcium binding, was reported to have a low affinity of 5–10 μM. Consequently, if 10–20 μM [Ca^{2+}] are not physiological, it would appear that cytosolic calcium would never rise to levels high enough to activate the MCU [47]. Nevertheless, the existence of microdomains of high calcium near the junction of mitochondria and the site of calcium release (the ER/SR) allows the activation of MCU and calcium uptake to occur. In mice, and due to substantially greater heart rates, cardiac mitochondria are expected to be exposed to even higher calcium levels. We therefore suggest that the selected pulsing concentrations of Ca^{2+} are physiological and provide relevant insight on cardiomyocytes in vivo.

We have identified that mitochondrial CRC in the heart is significantly higher during sleep as indicated by the delayed opening of the mPTP observed during the sleep period. Mitochondria isolated from hearts during sleep tended to accumulate larger amounts of Ca^{2+} before mPTP opening by Ca^{2+} overload. Our current results are consistent with another study showing circadian rhythmicity of gene and protein expressions of L-VGCCs, VGCCα1C (CaV1.2) and VGCCα1D (CaV1.3) in embryonic chick hearts [21]. The same study also showed a significantly higher average L-VGCC current density in cardiomyocytes when recordings were performed during the night than during the day. Multiple T-type Ca^{2+} channels as well as the ryanodine receptor have been shown to be under the control of the circadian clock in mice brains [21,37]. Circadian rhythmicity of intracellular Ca^{2+} has been verified within SCN of rodents [16–20] and Drosophila [49,49]. Moreover, circadian rhythmicity of Ca^{2+} release from mitochondria has been identified within SCN astrocytes and shown to be associated with fluctuations in extracellular ATP level [50].

To further investigate the relationship between circadian rhythmicity in mitochondrial Ca^{2+} dynamics observed in the present study and daily variations in circadian clock genes expressions we followed cardiac expression of the rhythmic clock genes *Bmal1* and *Per2* at ZG 0 and ZG 4. Our data indicate that cardiac expression of *Bmal1* was significantly lower at ZG 0 compared to ZG 4 with an opposite trend in the level of *Per2*. Noteworthy, opposite temporal trends for both *Bmal1* and *Per2* genes are well

documented not only in the SCN and liver, but also in the mouse heart and skeletal muscles [51]. Within cardiomyocytes, oscillations in circadian clock gene expression have been demonstrated and found to mediate variations in cardiac function and dysfunction over the course of the day. Expression levels of *Cry2*, *Per1*, and *Per2* peaked at the light-to- dark phase transition, whereas *Bmal1* and *Npas2* expression levels were significantly lower at the light-to-dark phase transition in the rat heart [52]. We also observed an increase in mitochondrial gene *ND1* on light-to-dark phase transition indicating that mitochondrial biogenesis may be altered between ZG 0 to ZG 4. Taken together, our findings suggest a diurnal rhythmicity of mitochondrial Ca^{2+} dynamics within murine heart which may be associated with oscillations in cardiac expressions of circadian clock genes.

The interplay between mitochondrial Ca^{2+} uptake, sequestration, and release is pivotal for the multiple physiological functions including bioenergetic elasticity and cell fate in response to stress. Mitochondrial Ca^{2+} accumulation was repeatedly shown to depend on a complex composed of an inner-membrane channel containing MCU and regulatory subunits including MICU1, MICU2, MCUb, EMRE, and MCU1. An emerging picture is consenting on a dual role for MICU1 [e.g. [54,54]; reviewed in[55]] and MICU2 [55] in regulating MCU channel depending on level of calcium. At resting cytosolic [Ca^{2+}], which is approximately 0.1 μM, MICU1 is free of Ca^{2+} and keeps the MCU channel closed. Upon cell stimulation, cytosolic [Ca^{2+}] rises and Ca^{2+} binds to MICU1, inducing MICU1 conformational changes and eventually MCU activation [56]. As a result, MCU exhibits low activity at resting cytosolic Ca^{2+} concentrations, but under Ca^{2+} overload is activated by a regulatory interaction with MICU1 [33].

Mitochondrial Ca^{2+} uptake behavior for a population of mitochondria within a tissue was elegantly shown to be dictated by the relative abundance of MICU1 and MCU [36]. In the present work, we found that the MICU1:MCU protein ratio decreased significantly on going from wake to sleep. It has been found that lower MICU1:MCU ratio, such as when comparing heart tissue with liver, was associated with lower threshold for calcium uptake, decreased cytosolic calcium, but also decreased cooperativity of uniporter activation. The trend towards lower ratio on the onset of sleep indicate relative abundance of MICU1-free uniporters that maybe compared with MICU1 loss of function or down-regulation/knock-out leading to disease phenotype including muscle weakness and myofiber regeneration [57] or even prenatal mortality [58]. Ironically, MICU1:MCU ratios estimated from mRNA expression levels showed a trend towards higher ratio during sleep. This may reflect the often reported transcription/translation discrepancy and may also reflect a dynamic cellular response to combat the opposite trend.

On the other hand, CypD is the major calcium sensor and essential for opening of the high-conductance channel mPTP [35,35]. Although *MCU* gene expression was not dependent on the time, MCU protein level was found to significantly increase at ZG4. Both *MICU1* gene and MICU2 protein expressions were significantly higher during sleep relative to wake time, which may explain the faster Ca^{2+} uptake during this period. Interestingly, quantification of *CypD* gene, revealed lower levels of expression during sleep relative to wake cycle. Consequently, one may propose that the higher rates of Ca^{2+}uptake observed during sleep period, are a consequence of higher level of expression of MCU while the delay in opening of mPTP and subsequent Ca^{2+} accumulation in mitochondria may reflect lower levels of expression of *CypD* genes during sleep. Western blot analysis indicated that the level of NCLX protein is significantly higher at ZG4. Although NCLX is a major calcium efflux channel, its activity was found to be highly sensitive to mild fluctuations in $\Delta\Psi_m$ [59].

In cardiomyocytes, the coupling of Ca^{2+} dynamics with mitochondrial bioenergetics is implicated in myocardial physiology and pathology [60]. Cardiac mitochondria exhibited significantly lower transmembrane potential during sleep period relative to wake period, consistent with earlier studies showing diurnal variations in myocardial oxygen consumption, carbohydrate oxidation and metabolic gene expression in isolated working rat heart, with a peak during the night (active phase) [62,62]. Circadian clock involvement in regulation of cardiac metabolism has also been previously reported. A study performed by Bray et al. 2008 using cardiomyocyte-specific circadian clock mutant mouse showed attenuation of state 3 mitochondrial respiration in subsarcolemmal mitochondrial fraction of the heart [63]. Bmal1 knockdown in mouse heart down-regulated expression of genes related to electron transport chain (ETC) and the tricarboxylic acid (TCA) cycle, and attenuated complex I activity [11]. This may explain the observed increase in *ND*1 gene expression in parallel with *Bmal*1 gene during sleep.

Mitochondrial respiration and ROS generation are interconnected [24,25,64]. In the fed state, a decrease in mitochondrial OXPHOS may result in highly reduced ETC components, which are more likely to leak electrons to molecular oxygen [26,65]. Indeed, our results revealed that the rate of H_2O_2 production during OXPHOS-I + II in cardiac mitochondria is significantly higher during sleep relative to wake period. In addition to the rhythmicity of OXPHOS in the diurnal fluctuations in ROS production, circadian clocks have been also suggested to influence mitochondrial ROS production. An increase in superoxide levels has been detected in primary hepatocytes from Bmal1-depleted murine liver [66]. Circadian rhythmicity of superoxide dismutase 2 (SOD2) acetylation and activity, which is responsible for the dismutation of superoxide into H_2O_2 is hindered in liver of mice with the ClockΔ19 mutation [67].

It is increasingly reported that Ca^{2+} homeostasis and ROS production are mutually interlinked. ROS can significantly affect Ca^{2+} homeostasis in the cell and vice versa. Excessive ROS are shown to be harmful and cause Ca^{2+} overload [69,70]. We therefore investigated if quercetin could quench ROS production in heart homogenate and block calcium uptake in freshly isolated mitochondria. Although with unclear mechanism, several reports indicated beneficial effects of quercetin in cardiovascular diseases, such as atherosclerosis, ischemia–reperfusion injury, cardiotoxicity, and hypertension, among others [e.g. reviewed in [70]]. In our hands, quercetin didn't significantly affect mitochondria respiration, but completely abolished hydrogen peroxide signal and mitochondrial calcium uptake. This may point at a remarkable interaction between mitochondrial ROS and calcium uptake. Nevertheless, our current findings confirmed an earlier study showing the effectiveness of quercetin against mitochondrial calcium accumulation, ROS production and opening of mPTP in rodent heart mitochondria in a model of aldosteronism [71]. Quercetin was also shown to exert a cardioprotective effect following hypoxia by suppressing post-hypoxic mitochondrial Ca^{2+} accumulation in h9c2 cardiomyocytes [38]. Prevention of ROS production and mitochondrial calcium sequestration by quercetin may alleviate the early stress vulnerability of the myocardium. We also compared time-of-the-day dependence of quercetin effect on mitochondrial responses to calcium pulsing. This analysis revealed that quercetin treatment of mitochondria isolated at ZG 4 was less protective against calcium overload for unknown reasons.

In summary, we provide functional and molecular data indicating that during sleep cardiac mitochondria exhibit faster calcium uptake while showing resistance to mPTP opening which may cause the inner respiratory machinery to be exposed to higher calcium levels. This may lead to lower OCR, lower transmembrane

potential, and greater ROS production. As a result, we suggest that during sleep, mitochondria are more stressed or prone to fail under cardiac insults. The mechanism proposed here to account for the often-reported time-of-the-day disparity in cardiac vulnerability to stress bears similarity with a mechanism suggested by Gandhi and co-workers to explain dysfunctional PTEN-induced kinase 1 (PINK1)-mediated vulnerability of neurons to cell death. Those authors found impaired Ca^{2+} efflux from mitochondria through the Na^{+}/Ca^{2+} exchanger in neurons lacking PINK1, a serine threonine kinase implicated in autosomal recessive early-onset parkinsonism. This was associated with increased Ca^{2+} uptake capacity, decreased membrane potential, and increased ROS production, all leading to neuronal death [72].

Conclusion

Taken together, we have detected diurnal fluctuations in mitochondrial calcium dynamics as well as mitochondrial bioenergetics and ROS production in murine hearts. Our study provides an evidence of mitochondrial Ca^{2+} overload during the sleep period. These changes were associated with attenuation in mitochondria-dependent OXPHOS and mitochondrial transmembrane potential, as well as increased ROS generation during sleep. Generally, the pathophysiological features of ischemic events involve accumulation of Ca^{2+} in the mitochondria, reduction in ATP production due to deficits in mitochondrial bioenergetics and oxidative stress, which are consistent with end of the sleep period. Blockade of this final process; e.g. using quercetin as we demonstrated here in isolated mitochondria, may assist in modulating diurnal risk and prevalence of cardiovascular events and inform therapeutic strategy.

Compliance with ethics requirements

All institutional and national guidelines for the care and use of animals were followed.

Declaration of Competing Interest

The authors declare the following financial interests/personal relationships which may be considered as potential competing interests: HHP has equity as a founder in CavoGene LifeSciences Holdings, LLC. All other authors have declared no conflict of interest.

Acknowledgements

This work was supported by a National Research Grant no. 6364 by the Science and Technology Development Fund, Egypt, awarded to SSA. SSA and EAA would like to acknowledge the support provided by Horizon 2020, COST Action CA15203 'MitoEAGLE'. This work was supported by grants from the National Institutes of Health (NIH) (HL091071, to H. H. Patel), and the Veterans Affairs (BX001963, to H. H. Patel). The authors thank Dr. Ali Mahmoud and Mr. Mahmoud Aboulsauod for their help in the transportation and maintenance of animals and for some technical help during this study. We are indebted to Dr. Moselhy R. Moselhy and Dr. Essam Abdel-Sattar of Cairo University for providing the pure quercetin used in this study. We also thank Dr. Ahmed A. El-Sifi for some technical help during his training in our laboratory.

Author contributions

EAA conducted metabolic studies, analyzed data and wrote the initial draft of the manuscript. SH conducted the calcium retention capacity study. AGA contributed to metabolic studies. MA, SHS, EEW, JPZ-H, HHP performed gene and protein determinations. BY along with AA and YR, NE and EE contributed to data analysis. NE conducted citrate synthase test. HG and HHP critically read the manuscript and provided advice regarding manuscript configuration. SSA perceived, designed, and supervised all studies in addition to analyzing data, interpreting results, and writing the manuscript in its final form. All authors revised the manuscript and approved its submission in the current form.

Appendix A. Supplementary material

Supplementary data to this article can be found online at https://doi.org/10.1016/j.jare.2021.01.006.

References

[1] Arı H, Sonmez O, Koc F, Demır K, Alıhanoglu Y, Ozdemır K, et al. Circadian rhythm of infarct size and left ventricular function evaluated with tissue Doppler echocardiography in ST elevation myocardial infarction. Hear Lung Circ 2016;25:250–6. doi: https://doi.org/10.1016/j.hlc.2015.06.833.
[2] Thosar SS, Butler MP, Shea SA. Role of the circadian system in cardiovascular disease. J Clin Invest 2018;128:2157–67. doi: https://doi.org/10.1172/JCI80590.
[3] Takeda N, Maemura K. Circadian clock and cardiovascular disease. J Cardiol 2011;57:249–56. doi: https://doi.org/10.1016/j.jjcc.2011.02.006.
[4] Takeda N, Maemura K. Circadian clock and the onset of cardiovascular events. Hypertens Res 2016;39:383–90. doi: https://doi.org/10.1038/hr.2016.9.
[5] Scheer FAJL, Hu K, Evoniuk H, Kelly EE, Malhotra A, Hilton MF, et al. Impact of the human circadian system, exercise, and their interaction on cardiovascular function. Proc Natl Acad Sci 2010;107:20541–6. doi: https://doi.org/10.1073/pnas.1006749107.
[6] Jones H, Atkinson G, Leary A, George K, Murphy M, Waterhouse J. Reactivity of ambulatory blood pressure to physical activity varies with time of day. Hypertension 2006;47:778–84. doi: https://doi.org/10.1161/01.HYP.0000206421.09642.b5.
[7] Scheer FAJL, Michelson AD, Frelinger AL, Evoniuk H, Kelly EE, McCarthy M, et al. The human endogenous circadian system causes greatest platelet activation during the biological morning independent of behaviors. PLoS ONE 2011;6:. doi: https://doi.org/10.1371/journal.pone.0024549e24549.
[8] Van Laake LW, Lüscher TF, Young ME. The circadian clock in cardiovascular regulation and disease: Lessons from the Nobel Prize in Physiology or Medicine 2017. Eur. Heart J. 2018;39:2326–9. doi: https://doi.org/10.1093/eurheartj/ehx775.
[9] Chen L, Yang G. Recent advances in circadian rhythms in cardiovascular system. Front Pharmacol 2015;6:71. doi: https://doi.org/10.3389/fphar.2015.00071.
[10] Young ME. Circadian control of cardiac metabolism: physiologic roles and pathologic implications. Methodist Debakey Cardiovasc J 2017;13:15–9. doi: https://doi.org/10.14797/mdcj-13-1-15.
[11] Kohsaka A, Das P, Hashimoto I, Nakao T, Deguchi Y, Gouraud SS, et al. The circadian clock maintains cardiac function by regulating mitochondrial metabolism in mice e112811. PLoS ONE 2014;9. doi: https://doi.org/10.1371/journal.pone.0112811.
[12] Martino TA, Young ME. Influence of the cardiomyocyte circadian clock on cardiac physiology and pathophysiology. J Biol Rhythms 2015;30:183–205. doi: https://doi.org/10.1177/0748730415575246.
[13] Javadov S, Karmazyn M, Escobales N. Mitochondrial permeability transition pore opening as a promising therapeutic target in cardiac diseases. J Pharmacol Exp Ther 2009;330:670–8. doi: https://doi.org/10.1124/jpet.109.153213.
[14] Dedkova EN, Blatter LA. Calcium signaling in cardiac mitochondria. J Mol Cell Cardiol 2013;58:125–33. doi: https://doi.org/10.1016/j.yjmcc.2012.12.021.
[15] Halestrap AP, Pasdois P. The role of the mitochondrial permeability transition pore in heart disease. Biochim Biophys Acta - Bioenerg 2009;1787:1402–15. doi: https://doi.org/10.1016/j.bbabio.2008.12.017.
[16] Enoki R, Ono D, Kuroda S, Honma S, Honma K-I. Dual origins of the intracellular circadian calcium rhythm in the suprachiasmatic nucleus. Sci Rep 2017;7:41733. doi: https://doi.org/10.1038/srep41733.
[17] Noguchi T, Leise TL, Kingsbury N, Diemer T, Wang LL, Henson MA, Welsh DK. Calcium circadian rhythmicity in the suprachiasmatic nucleus: cell autonomy and network modulation ENEURO.0160-17.2017. Eneuro 2017;4. doi: https://doi.org/10.1523/ENEURO.0160-17.2017.
[18] Colwell CS. Rhythmic coupling among cells in the suprachiasmatic nucleus. J Neurobiol 2000;43:379–88 (accessed January 9, 2019) http://www.ncbi.nlm.nih.gov/pubmed/10861563.
[19] Ikeda M, Sugiyama T, Wallace CS, Gompf HS, Yoshioka T, Miyawaki A, et al. Circadian dynamics of cytosolic and nuclear Ca2+ in single suprachiasmatic nucleus neurons. Neuron 2003;38:253–63 (accessed January 9, 2019) http://www.ncbi.nlm.nih.gov/pubmed/12718859.
[20] Enoki R, Kuroda S, Ono D, Hasan MT, Ueda T, Honma S, et al. Topological specificity and hierarchical network of the circadian calcium rhythm in the suprachiasmatic nucleus. Proc Natl Acad Sci U S A 2012;109:21498–503. doi: https://doi.org/10.1073/pnas.1214415110.

[21] Nordskog BK, Hammarback JA, Godwin DW. Diurnal gene expression patterns of T-type calcium channels and their modulation by ethanol. Neuroscience 2006;141:1365–73. doi: https://doi.org/10.1016/j.neuroscience.2006.04.031.
[22] Ko ML, Shi L, Grushin K, Nigussie F, Ko GY-P. Circadian profiles in the embryonic chick heart: L-type voltage-gated calcium channels and signaling pathways. Chronobiol Int 2010;27:1673–96. doi: https://doi.org/10.3109/07420528.2010.514631.
[23] Beesley S, Noguchi T, Welsh DK. Cardiomyocyte circadian oscillations are cell-autonomous, amplified by β-Adrenergic signaling, and synchronized in cardiac ventricle tissue. PLoS ONE 2016;11. doi: https://doi.org/10.1371/journal.pone.0159618.
[24] Abdel-Rahman EA, Mahmoud AM, Aaliya A, Radwan Y, Yasseen B, Al-Okda A, et al. Resolving contributions of oxygen-consuming and ROS-generating enzymes at the synapse 2016. Oxid Med Cell Longev 2016:1089364. doi: https://doi.org/10.1155/2016/1089364.
[25] Khalifa ARM, Abdel-Rahman EA, Mahmoud AM, Ali MH, Noureldin M, Saber SH, et al. Sex-specific differences in mitochondria biogenesis, morphology, respiratory function, and ROS homeostasis in young mouse heart and brain. Physiol Rep 2017;5. e13125.
[26] Gostimskaya IS, Grivennikova VG, Zharova TV, Bakeeva LE, Vinogradov AD. In situ assay of the intramitochondrial enzymes: use of alamethicin for permeabilization of mitochondria. Anal Biochem 2003;313:46–52 (accessed January 9, 2019) http://www.ncbi.nlm.nih.gov/pubmed/12576057.
[27] Laker RC, Taddeo EP, Akhtar YN, Zhang M, Hoehn KL, Yan Z. The mitochondrial permeability transition pore regulator cyclophilin D exhibits tissue-specific control of metabolic homeostasis e0167910. PLoS ONE 2016;11. doi: https://doi.org/10.1371/journal.pone.0167910.
[28] Mushrush DJ, Koteiche HA, Sammons MA, Link AJ, Mchaourab HS, Lacy DB. Studies of the mechanistic details of the pH-dependent association of botulinum neurotoxin with membranes. J Biol Chem 2011;286:27011–8. doi: https://doi.org/10.1074/jbc.M111.256982.
[29] Paredes RM, Etzler JC, Watts LT, Zheng W, Lechleiter JD. Chemical calcium indicators. Methods 2008;46:143–51. doi: https://doi.org/10.1016/j.ymeth.2008.09.025.
[30] Parnis J, Montana V, Delgado-Martinez I, Matyash V, Parpura V, Kettenmann H, et al. Mitochondrial exchanger NCLX plays a major role in the intracellular Ca2 + signaling, gliotransmission, and proliferation of astrocytes. J Neurosci 2013;33:7206–19. doi: https://doi.org/10.1523/JNEUROSCI.5721-12.2013.
[31] Ikeda M, Ikeda M. Bmal1 is an Essential regulator for circadian cytosolic Ca2+ rhythms in suprachiasmatic nucleus neurons. J Neurosci 2014;34:12029–38. doi: https://doi.org/10.1523/JNEUROSCI.5158-13.2014.
[32] Martino TA, Tata N, Belsham DD, Chalmers J, Straume M, Lee P, et al. Disturbed diurnal rhythm alters gene expression and exacerbates cardiovascular disease with rescue by resynchronization. Hypertension 2007;49:1104–13. doi: https://doi.org/10.1161/HYPERTENSIONAHA.106.083568.
[33] Patron M, Checchetto V, Raffaello A, Teardo E, Vecellio Reane D, Mantoan M, et al. MICU1 and MICU2 finely tune the mitochondrial Ca2+ uniporter by exerting opposite effects on MCU activity. Mol Cell 2014;53:726–37. doi: https://doi.org/10.1016/j.molcel.2014.01.013.
[34] Basso E, Fante L, Fowlkes J, Petronilli V, Forte MA, Bernardi P. Properties of the permeability transition pore in mitochondria devoid of Cyclophilin D. J Biol Chem 2005;280:18558–61. doi: https://doi.org/10.1074/jbc.C500089200.
[35] Baines CP, Kaiser RA, Purcell NH, Blair NS, Osinska H, Hambleton MA, et al. Loss of cyclophilin D reveals a critical role for mitochondrial permeability transition in cell death. Nature 2005;434:658–62. doi: https://doi.org/10.1038/nature03434.
[36] Paillard M, Csordás G, Szanda G, Golenár T, Debattisti V, Bartok A, et al. Tissue-specific mitochondrial decoding of cytoplasmic Ca2+ signals is controlled by the stoichiometry of MICU1/2 and MCU. Cell Rep 2017;18:2291–300. doi: https://doi.org/10.1016/j.celrep.2017.02.032.
[37] Pfeffer M, Müller CM, Mordel J, Meissl H, Ansari N, Deller T, et al. The mammalian molecular clockwork controls rhythmic expression of its own input pathway components. J Neurosci 2009;29:6114–23. doi: https://doi.org/10.1523/JNEUROSCI.0275-09.2009.
[38] Zholobenko AV, Mouithys-Mickalad A, Dostal Z, Serteyn D, Modriansky M. On the causes and consequences of the uncoupler-like effects of quercetin and dehydrosilybin in H9c2 cells e0185691. PLoS ONE 2017;12. doi: https://doi.org/10.1371/journal.pone.0185691.
[39] Panickar KS, Anderson RA. Mechanisms underlying the protective effects of myricetin and quercetin following oxygen-glucose deprivation-induced cell swelling and the reduction in glutamate uptake in glial cells. Neuroscience 2011;183:1–14. doi: https://doi.org/10.1016/j.neuroscience.2011.03.064.
[40] Demeter-Haludka V, Kovács M, Prorok J, Nagy N, Varró A, Végh Á. Examination of the changes in calcium homeostasis in the delayed antiarrhythmic effect of sodium nitrite. Int J Mol Sci 2019;20. doi: https://doi.org/10.3390/ijms20225687.
[41] Mishra J, Davani AJ, Natarajan GK, Kwok WM, Stowe DF, Camara AKS. Cyclosporin A increases mitochondrial buffering of calcium: an additional mechanism in delaying mitochondrial permeability transition pore opening. Cells 2019;8. doi: https://doi.org/10.3390/cells8091052.
[42] Azzolin L, Antolini N, Calderan A, Ruzza P, Sciacovelli M, Marin O, et al. Antamanide, a derivative of amanita phalloides, is a novel inhibitor of the mitochondrial permeability transition pore. PLoS ONE 2011;6. doi: https://doi.org/10.1371/journal.pone.0016280.
[43] Leddy HA, McNulty AL, Guilak F, Liedtke W. Unraveling the mechanism by which TRPV4 mutations cause skeletal dysplasias. Rare Dis 2014;2:. doi: https://doi.org/10.4161/2167549X.2014.962971e962971.
[44] Odinokova I, Baburina Y, Kruglov A, Fadeeva I, Zvyagina A, Sotnikova L, et al. Effect of melatonin on rat heart mitochondria in acute heart failure in aged rats. Int J Mol Sci 2018;19. doi: https://doi.org/10.3390/ijms19061555.
[45] Marks AR. Calcium and the heart: A question of life and death. J Clin Invest 2003;111:597–600. doi: https://doi.org/10.1172/JCI18067.
[46] Williams GSB, Boyman L, Chikando AC, Khairallah RJ, Lederer WJ. Mitochondrial calcium uptake. Proc Natl Acad Sci U S A 2013;110:10479–86. doi: https://doi.org/10.1073/pnas.1300410110.
[47] Finkel T, Menazza S, Holmström KM, Parks RJ, Liu J, Sun J, et al. The ins and outs of mitochondrial calcium. Circ Res 2015;116:1810–9. doi: https://doi.org/10.1161/CIRCRESAHA.116.305484.
[48] Liang X, Holy TE, Taghert PH. Synchronous Drosophila circadian pacemakers display nonsynchronous Ca^{2+} rhythms in vivo. Science 2016;351:976–81. doi: https://doi.org/10.1126/science.aad3997.
[49] Brancaccio M, Patton AP, Chesham JE, Maywood ES, Hastings MH. Astrocytes control circadian timekeeping in the suprachiasmatic nucleus via glutamatergic signaling. Neuron 2017;93:1420–1435.e5. doi: https://doi.org/10.1016/j.neuron.2017.02.030.
[50] Burkeen JF, Womac AD, Earnest DJ, Zoran MJ. Mitochondrial calcium signaling mediates rhythmic extracellular ATP accumulation in suprachiasmatic nucleus astrocytes. J Neurosci 2011;31:8432–40. doi: https://doi.org/10.1523/JNEUROSCI.6576-10.2011.
[51] Schiaffino S, Blaauw B, Dyar KA. The functional significance of the skeletal muscle clock: lessons from Bmal1 knockout models. Skelet Muscle 2016;6:33. doi: https://doi.org/10.1186/s13395-016-0107-5.
[52] Young ME. The circadian clock within the heart: potential influence on myocardial gene expression, metabolism, and function. Am J Physiol Circ Physiol 2006;290:H1–H16. doi: https://doi.org/10.1152/ajpheart.00582.2005.
[53] Csordás G, Golenár T, Seifert EL, Kamer KJ, Sancak Y, Perocchi F, et al. MICU1 controls both the threshold and cooperative activation of the mitochondrial Ca2+ uniporter. Cell Metab 2013;17:976–87. doi: https://doi.org/10.1016/j.cmet.2013.04.020.
[54] Paillard M, Csordás G, Huang KT, Várnai P, Joseph SK, Hajnóczky G. MICU1 interacts with the D-Ring of the MCU pore to control its Ca2+ flux and sensitivity to Ru360. Mol Cell 2018;72:778–785.e3. doi: https://doi.org/10.1016/j.molcel.2018.09.008.
[55] Mammucari C, Gherardi G, Rizzuto R. Structure, activity regulation, and role of the mitochondrial calcium uniporter in health and disease. Front Oncol 2017;7. doi: https://doi.org/10.3389/fonc.2017.00139.
[56] Wang L, Yang X, Li S, Wang Z, Liu Y, Feng J, et al. Structural and mechanistic insights into MICU1 regulation of mitochondrial calcium uptake. EMBO J 2014;33:594–604. doi: https://doi.org/10.1002/embj.201386523.
[57] Logan CV, Szabadkai G, Sharpe JA, Parry DA, Torelli S, Childs AM, et al. Loss-of-function mutations in MICU1 cause a brain and muscle disorder linked to primary alterations in mitochondrial calcium signaling. Nat Genet 2014;46:188–93. doi: https://doi.org/10.1038/ng.2851.
[58] Antony AN, Paillard M, Moffat C, Juskeviciute E, Correnti J, Bolon B, et al. MICU1 regulation of mitochondrial Ca 2+ uptake dictates survival and tissue regeneration. Nat Commun 2016;7. doi: https://doi.org/10.1038/ncomms10955.
[59] Kostic M, Katoshevski T, Sekler I. Allosteric regulation of NCLX by mitochondrial membrane potential links the metabolic state and Ca2+ signaling in mitochondria. Cell Rep 2018;25:3465–3475.e4. doi: https://doi.org/10.1016/j.celrep.2018.11.084.
[60] Das PN, Pedruzzi G, Bairagi N, Chatterjee S. Coupling calcium dynamics and mitochondrial bioenergetic: an in silico study to simulate cardiomyocyte dysfunction. Mol Biosyst 2016;12:806–17. doi: https://doi.org/10.1039/C5MB00872G.
[61] Stavinoha MA, RaySpellicy JW, Hart-Sailors ML, Mersmann HJ, Bray MS, Young ME. Diurnal variations in the responsiveness of cardiac and skeletal muscle to fatty acids. Am J Physiol Metab 2004;287:E878–87. doi: https://doi.org/10.1152/ajpendo.00189.2004.
[62] Young ME, Razeghi P, Cedars AM, Guthrie PH, Taegtmeyer H. Intrinsic diurnal variations in cardiac metabolism and contractile function. Circ Res 2001;89:1199–208. doi: https://doi.org/10.1161/hh2401.100741.
[63] Bray MS, Shaw CA, Moore MWS, Garcia RAP, Zanquetta MM, Durgan DJ, et al. Disruption of the circadian clock within the cardiomyocyte influences myocardial contractile function, metabolism, and gene expression. Am J Physiol Circ Physiol 2008;294:H1036–47. doi: https://doi.org/10.1152/ajpheart.01291.2007.
[64] Kolamunne RT, Dias IHK, Vernallis AB, Grant MM, Griffiths HR. Nrf2 activation supports cell survival during hypoxia and hypoxia/reoxygenation in cardiomyoblasts; the roles of reactive oxygen and nitrogen species. Redox Biol 2013;1:418–26. doi: https://doi.org/10.1016/j.redox.2013.08.002.
[65] Cuddihy SL, Ali SS, Musiek ES, Lucero J, Kopp SJ, Morrow JD, et al. Prolonged alpha-tocopherol deficiency decreases oxidative stress and unmasks alpha-tocopherol-dependent regulation of mitochondrial function in the brain. J Biol Chem 2008;283:6915–24. doi: https://doi.org/10.1074/jbc.M702572200.
[66] Jacobi D, Liu S, Burkewitz K, Kory N, Knudsen NH, Alexander RK, et al. Hepatic Bmal1 regulates rhythmic mitochondrial dynamics and promotes metabolic fitness. Cell Metab 2015;22:709–20. doi: https://doi.org/10.1016/j.cmet.2015.08.006.

[67] Gong C, Li C, Qi X, Song Z, Wu J, Hughes ME, et al. The daily rhythms of mitochondrial gene expression and oxidative stress regulation are altered by aging in the mouse liver. Chronobiol Int 2015;32:1254–63. doi: https://doi.org/10.3109/07420528.2015.1085388.
[68] Yan Y, Wei C, Zhang W, Cheng H, Liu J. Cross-talk between calcium and reactive oxygen species signaling. Acta Pharmacol Sin 2006;27:821–6. doi: https://doi.org/10.1111/j.1745-7254.2006.00390.x.
[69] Görlach A, Bertram K, Hudecova S, Krizanova O. Calcium and ROS: A mutual interplay. Redox Biol 2015;6:260–71. doi: https://doi.org/10.1016/j.redox.2015.08.010.
[70] Gormaz JG, Quintremil S, Rodrigo R. Cardiovascular disease: A target for the pharmacological effects of quercetin. Curr Top Med Chem 2015;15:1735–42 (accessed June 11, 2019) http://www.ncbi.nlm.nih.gov/pubmed/25915608.
[71] Shahbaz AU, Kamalov G, Zhao W, Zhao T, Johnson PL, Sun Y, et al. Mitochondria-targeted cardioprotection in aldosteronism. J Cardiovasc Pharmacol 2011;57:37–43. doi: https://doi.org/10.1097/FJC.0b013e3181fe1250.
[72] Gandhi S, Wood-Kaczmar A, Yao Z, Plun-Favreau H, Deas E, Klupsch K, et al. PINK1-associated Parkinson's disease is caused by neuronal vulnerability to calcium-induced cell death. Mol Cell 2009;33:627–38. doi: https://doi.org/10.1016/j.molcel.2009.02.013.